Mechanism and Machine Theory 87 (2015) 45–56

Contents lists available at ScienceDirect

Mechanism and Machine Theory

journal homepage: www.elsevier.com/locate/mechmt

Analysis of the displacement amplification ratio of bridge-type mechanism

Ke-qi Qi [a,*], Yang Xiang [a], Chao Fang [a], Yang Zhang [b], Chang-song Yu [a]

[a] Changchun Institute of Optics, Fine Mechanics and Physics, Chinese Academy of Science, Dong_Nanhu Road 3888, Changchun, Jilin 130033, PR China
[b] Shenyang Institute of Automation, Chinese Academy of Science, No. 114 Nanta Road, Shenhe District, Shenyang, Liaoning 11016, PR China

ARTICLE INFO

Article history:
Received 28 December 2013
Received in revised form 12 December 2014
Accepted 25 December 2014
Available online 10 January 2015

Keywords:
Bridge-type mechanism
Displacement amplification ratio
Kinematic theory
Elastic beam theory
Finite element method (FEM)

ABSTRACT

In order to further understand the characteristics of displacement amplification of bridge-type mechanism, specific analysis is presented in this paper. The average ideal displacement amplification ratio during the deformation process is obtained based on the kinematics theories. Elastic beam theory is adopted to analyze the deformation of the hinges, and a novel formula of theoretical displacement amplification ratio is carried out. A conclusion is reached that the displacement amplification ratio is not related to the material and thickness of structure. Moreover, this conclusion is verified by finite element method. The relationship between displacement amplification ratio and the structural dimensions is analyzed in depth. After the comparisons with existing methods, the formula obtained by elastic beam theory in this paper is proved to be more reliable. And this conclusion is confirmed by the comparison with previous experiment. Furthermore, the influence of geometric nonlinearity of bridge-type mechanism is also well analyzed.

1. Introduction

Due to the characteristics of high force, high stiffness, high resolution and fast response, piezostack is a typical actuator for ultra-precision motion and positioning [1–4]. A major drawback of conventional piezostack, which limits its applications, is its relatively small deformation range. Generally, the deformation range of piezostack is about 0.1% of its own length [5,6]. In most of its applications, larger working ranges are required. Therefore, amplification mechanisms are needed. Flexure-based compliant mechanism is the first choice, which has no backlash, no lubrication requirement, repeatable motion and vacuum compatibility [7–10]. Lever-type mechanism is the most common one [11,12]. In addition, bridge-type, four-bar linkage and Scott-Russell mechanisms are also frequently used [13–17]. Comparing to the traditional amplifiers, bridge-type mechanism has a compact structure and a large displacement amplification ratio. Therefore, bridge-type mechanism becomes more and more popular in modern industry.

So far, there are many different types of flexure hinges have been developed, such as right-circular, elliptical, parabolic, right-angle, hyperbolic, V-shaped, cycloidal, corner-filleted and hybrid flexure hinges [18–20]. Different profile has different performance and characteristics. Generally, the right-circular hinge profile has the highest stiffness, and the right-angle hinge profile has the lowest stiffness. In the paper, right-angle hinge was adopted.

Pokines and Garcia [21] analyzed the relationship between the ideal displacement amplification ratio of bridge-type mechanism and the angular variation of bridge arm, as he designed and fabricated a MEMS-type micro-amplification device. Lobontiu and Garcia [22] analyzed the relationship between the ideal displacement amplification ratio of bridge-type mechanism and input displacement. In the same paper, Lobontiu and Garcia also derived stiffness and displacement formulas of bridge-type mechanism based on the principle of strain energy and Castigliano's second theorem, but these formulas are too complicated and lack of practicality.

* Corresponding author. Tel.: +86 186 4311 6163; fax: +86 0431 8617 6138.
E-mail address: qikeqi1985@126.com (K. Qi).

http://dx.doi.org/10.1016/j.mechmachtheory.2014.12.013
0094-114X/

Ma et al. [13] derived the ideal displacement amplification ratio of bridge-type mechanism using kinematic theory, and derived the theoretic displacement amplification ratio using virtual work principle. However, the output displacement was obtained by geometric relations, and its elastic deformation was not considered. So, this theoretic formula is not consummate. Ye et al. [23] derived the theoretic displacement amplification ratio of bridge-type mechanism using kinematic principle and elastic beam theory, but he neglected the tensile deformation and deflection of hinges. In this paper, the kinematic characteristics of bridge-type mechanism are deeply analyzed, and a new theoretic displacement amplification ratio formula is derived based on elastic beam theory. Meanwhile, the relationships between displacement amplification ratio and the material and dimensions of the structure are analyzed. According to the analysis, a conclusion is reached that the displacement amplification ratio of bridge-type mechanism is not related to the material and thickness of the structure, and it is verified by finite element analysis (FEA). After comparisons with all mentioned methods, the new formula is proved to be more reliable. In order to confirm this conclusion, comparison with previous experimental results has also been made. Because of the geometric nonlinearity of bridge-type mechanism, nonlinear static analysis is taken. And the influence from input displacement to displacement amplification ratio is well analyzed.

2. Kinematic analysis of bridge-type mechanism

The schematic of bridge-type mechanism is depicted in Fig. 1. From Fig. 1, it is easy to obtain that the displacement amplification ratio of bridge-type mechanism is the ratio of output displacement to input displacement, and the input displacement is actually the elongation of piezostack. Before the kinematic analysis is taken, the bridge-type mechanism requires to be simplified into an ideal multi-rigid body mechanism with ideal pivots, as shown in Fig. 2. Because of the double symmetrical structure, only one arm of the mechanism is needed to be analyzed. Fig. 3 shows the one quarter-model of the mechanism.

Pokines and Garcia [21] derived the ideal displacement amplification ratio of bridge-type mechanism from the angular variation of bridge arm:

$$R_{amp} = \left| \frac{\sin\alpha - \sin(\alpha - \Delta\alpha)}{\cos\alpha - \cos(\alpha - \Delta\alpha)} \right| \tag{1}$$

Lobontiu and Garcia [22] derived the ideal displacement amplification ratio of bridge-type mechanism using geometric relations of the input displacement and output displacement:

$$R_{amp} = \frac{\sqrt{L_a^{\,2} \cdot \sin^2\alpha - 2L_a \cdot \Delta L_1 \cdot \cos\alpha - \Delta L_1^{\,2}} + L_a \cdot \sin\alpha}{\Delta L_1} \tag{2}$$

Ma et al. [13] analyzed the instantaneous velocity of bridge-type mechanism, and derived the ideal displacement amplification ratio of bridge-type mechanism using kinematic relations:

$$R_{amp} = \frac{\partial y}{\partial x} = \frac{\partial y/\partial t}{\partial x/\partial t} = \frac{\omega \cdot L_1}{\omega \cdot h} = \cot\alpha \tag{3}$$

Actually, Eq. (3) represents the transient expression of Eq. (1) [13]. Deformation is a dynamic process, so the displacement amplification ratio is a dynamic value in the procedure of deformation. Then, the even displacement amplification ratio of the whole procedure of deformation is

$$R_{amp} = \frac{\int_{\alpha-\Delta\alpha}^{\alpha} \cot x dx}{\Delta\alpha} = \frac{\ln\left(\frac{\sin\alpha}{\sin(\alpha-\Delta\alpha)}\right)}{\Delta\alpha} \tag{4}$$

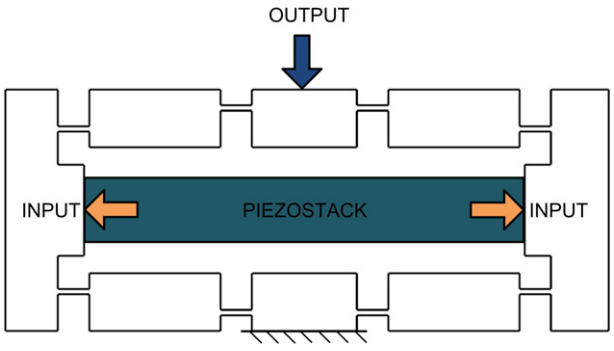

Fig. 1. Schematic of bridge-type displacement amplification mechanism.

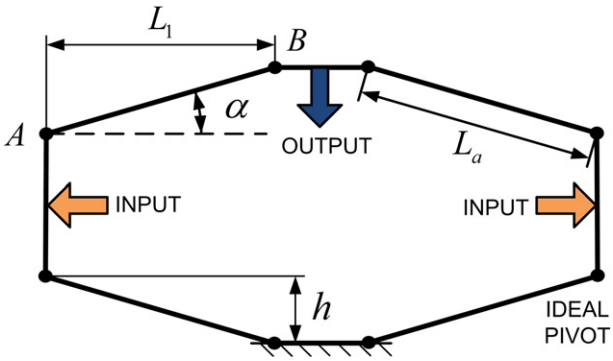

Fig. 2. Schematic of ideal model of bridge-type mechanism.

Based on geometric relations, the following relationship can be obtained when the deformation is small:

$$\Delta\alpha \approx \frac{\Delta x}{L_a \sin\alpha} \tag{5}$$

where Δx denotes the input displacement. Therefore, Eq. (4) can be written as:

$$R_{amp\_ideal} = \frac{h \cdot \left[\ln\left(\frac{h}{\sqrt{h^2 + {L_1}^2}} \right) - \ln\left(\sin\left(\arctan\left(\frac{h}{L_1} \right) - \frac{\Delta x}{h} \right) \right) \right]}{\Delta x} \tag{6}$$

Actually, if the input displacement is relatively large, Eq. (6) is more accurate than Eq. (3); or else, the difference between Eq. (3) and Eq. (6) could be ignored.

3. Analysis based on elastic beam theory

There are too many simplifications in the above analysis, such as the deformation of flexure hinges is ignored. Otherwise, the material properties may also influence the displacement amplification ratio of bridge-type mechanism. So, analysis based on elastic beam theory is taken in this section.

Since the big differences of topology, each arm of the bridge-type mechanism can be regarded as a rigid link connecting two flexure hinges, and the flexure hinge can be regarded as an elastic beam. By the same token, only a quarter of the elastic model is needed to be analyzed, as shown in Fig. 4.

From the force equilibrium theory, it is easy to get that $F_A = F_B$ and $2M_A = 2M_B = F_A \cdot h$. In order to simplify the expression, make $F_A = F_B = F$ and $M_A = M_B = M$. Fig. 5 shows elastic deformation of quarter model of bridge-type mechanism. Then, the displacement amplification ratio of bridge-type mechanism can be written as:

$$R_{amp} = \frac{2\Delta y}{2\Delta x} = \frac{\Delta y}{\Delta x} \tag{7}$$

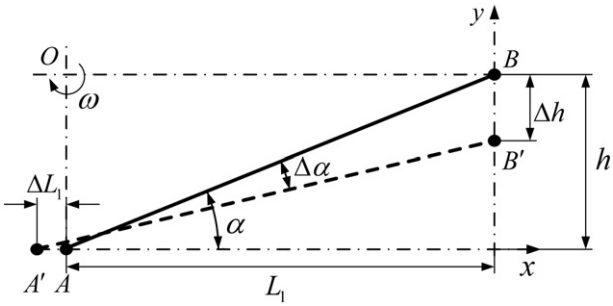

Fig. 3. Quarter of ideal model of bridge-type mechanism.

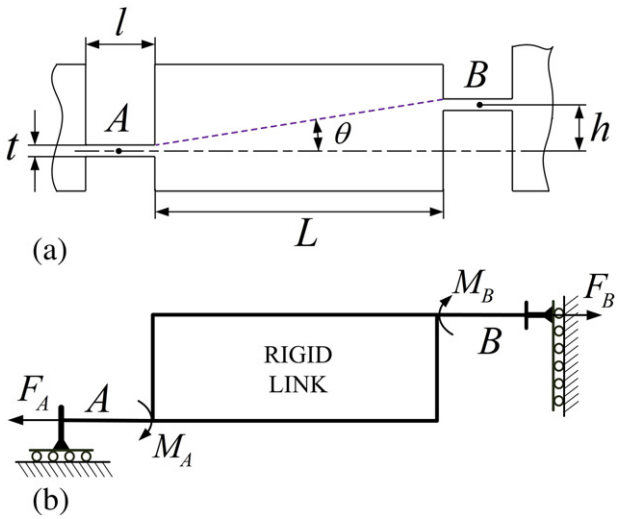

Fig. 4. Quarter of elastic model of bridge-type mechanism.

Furthermore, a certain angle of rotation is occurred both in the flexure hinges and rigid link. Fig. 6 shows the local detail of rotation of bridge-type mechanism. According to the Euler–Bernoulli beam theory, the cross-sectional plane of deformed beam is still perpendicular to the deformed axis, and one can derive that:

$$\Delta\theta = \Delta\theta_l \tag{8}$$

So, $\Delta\theta$ can be obtained from the rotation of flexure hinges. In addition, flexure hinges A and B have the same angle of rotation, because of the same force status. Fig. 7 shows the force status and deformation of flexure hinge A.

As shown in Fig. 7, flexure hinge A can be considered as a cantilever. Based on the elastic beam theory, the following relation can be obtained:

$$\Delta x_l = \frac{F}{K_l}, \Delta\theta_l = \frac{M}{K_\theta} = \frac{Fh}{2K_\theta}, \Delta y_l = \frac{Ml}{2K_\theta} = \frac{Flh}{4K_\theta} \tag{9}$$

where K_l and K_θ denote the translational stiffness and the rotational stiffness of right-angle flexure hinge, respectively.

Comparing with its dimensions, the deformation of bridge-type mechanism is generally very small. That is to say $\Delta\theta$ is very small. So, the chord length generated by rotation of the rigid body approximately equals to the arc length corresponding to $\Delta\theta$. Then, the following relationship can be derived:

$$\begin{cases} \Delta x = 2\Delta x_l + \sqrt{L^2 + h^2} \cdot \Delta\theta \cdot \sin\theta = 2\Delta x_l + h \cdot \Delta\theta \\ \Delta y = 2\Delta y_l + \sqrt{L^2 + h^2} \cdot \Delta\theta \cdot \cos\theta = 2\Delta y_l + L \cdot \Delta\theta \end{cases} \tag{10}$$

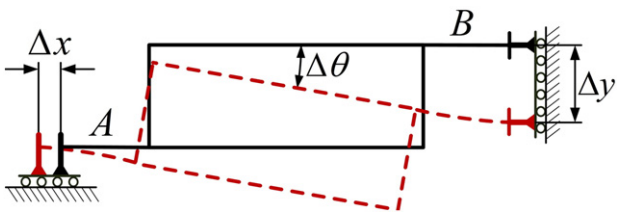

Fig. 5. Elastic deformation of quarter model of bridge-type mechanism.

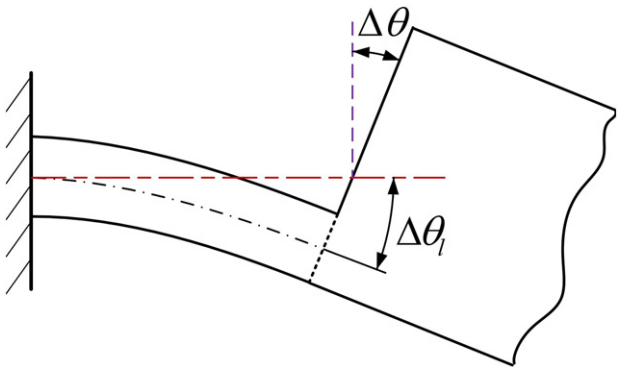

Fig. 6. Local detail of rotation of bridge-type mechanism.

From Eqs. (7) and (10), the displacement amplification ratio can be expressed as:

$$R_{amp} = \frac{\Delta y}{\Delta x} = \frac{2\Delta y_l + L \cdot \Delta\theta}{2\Delta x_l + h \cdot \Delta\theta} \tag{11}$$

In view of Eqs. (8) and (9), Eq. (11) can be further written as:

$$R_{amp} = \frac{\Delta y}{\Delta x} = \frac{\dfrac{Flh}{2K_\theta} + L \cdot \dfrac{Fh}{2K_\theta}}{\dfrac{2F}{K_l} + h \cdot \dfrac{Fh}{2K_\theta}} = \frac{lh \cdot K_l + Lh \cdot K_l}{4K_\theta + h^2 \cdot K_l} \tag{12}$$

In the literature, stiffness of different types of flexure hinges has been derived. Koseki et al. [16,24] derived the compliance matrix of the flexure hinge from beam theory. The hinge compliance equation is as follows:

$$X = CF \tag{13}$$

$$F = KX \tag{14}$$

where

$$X = [\Delta x \quad \Delta y \quad \Delta z \quad \Delta\alpha \quad \Delta\beta \quad \Delta\gamma]^T$$
$$F = [F_x \quad F_y \quad F_z \quad M_x \quad M_y \quad M_z]^T$$

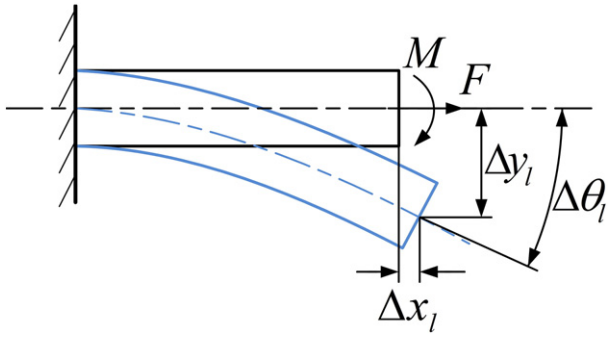

Fig. 7. Force status and deformation of right-angle flexure hinge.

The matrix C is the compliance matrix of flexure hinge, and K is the stiffness matrix of flexure hinge. It is obvious that C and K are inverse matrix of each other. The compliance matrix of right-angle flexure hinge is as follows:

$$C = \begin{bmatrix} \frac{l}{Ebt} & 0 & 0 & 0 & 0 & 0 \\ 0 & \frac{4l^3}{3Ebt^3} + \frac{l}{Gbt} & 0 & 0 & 0 & \frac{6l^2}{Ebt^3} \\ 0 & 0 & \frac{4l^3}{3Eb^3t} + \frac{l}{Gbt} & 0 & -\frac{6l^2}{Eb^3t} & 0 \\ 0 & 0 & 0 & \frac{l}{Gk_2bt^3} & 0 & 0 \\ 0 & 0 & -\frac{6l^2}{Eb^3t} & 0 & \frac{12l}{Eb^3t} & 0 \\ 0 & \frac{6l^2}{Ebt^3} & 0 & 0 & 0 & \frac{12l}{Ebt^3} \end{bmatrix} \tag{15}$$

where E is the elastic modulus, G is the shear modulus of hinge material, and k_2 is a geometrical constant determined by b/t [16,24]. The coordinate system of the right-angle hinge is shown in Fig. 8.

Only the planar stiffness needs to be considered for a bridge-type mechanism. So, K_l and $K_{\theta\ \text{can be derived}}$ from Eq. (15) as follow:

$$K_l = \frac{Ebt}{l},\ K_\theta = \frac{Ebt^3}{12l} \tag{16}$$

From Eqs. (12) and (16)

$$R_{amp\_elastic} = \frac{\Delta y}{\Delta x} = \frac{lh \cdot \frac{Ebt}{l} + hL \cdot \frac{Ebt}{l}}{4 \cdot \frac{Ebt^3}{12l} + h^2 \cdot \frac{Ebt}{l}} = \frac{3h(l+L)}{t^2 + 3h^2} \tag{17}$$

From Eq. (17), it can be seen that the displacement amplification ratio of bridge-type mechanism is not related to the material and thickness of the structure. We can also find that the displacement amplification ratio is not related to the length of L or l, when the horizontal distance between the centers of hinges (L_1 in Fig. 2 or $L + l$ in Fig. 4a) is fixed.

Fig. 10 shows the relationship between displacement amplification ratio and structural dimensions. And the structural dimensions of the bridge-type mechanism are shown in Fig. 9.

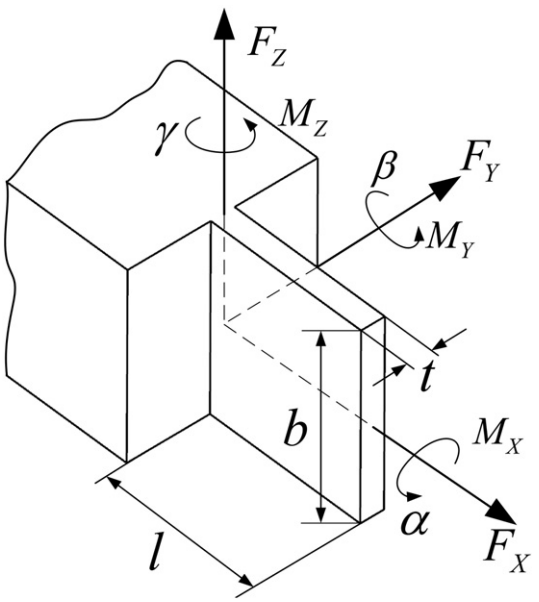

Fig. 8. Coordinate system of right-angle flexure hinge.

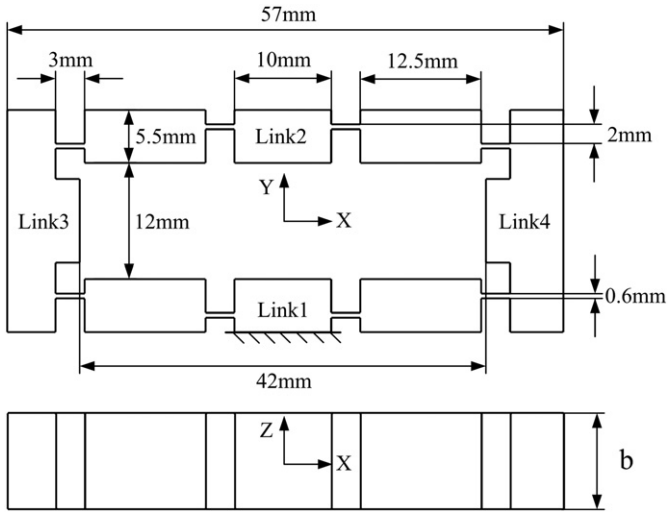

Fig. 9. Structural dimensions of bridge-type mechanism.

4. Comparison of different materials and thicknesses

To verify the conclusion that the amplification ratio of bridge-type mechanism is not related to the material and thickness (*b* in Fig. 9) of the structure, FEA is carried out in this section. The FEA is realized by commercial software ANSYS11.0, and solid45 element is chosen to build the model. Most of the elements are hexahedron elements, and some prism-shaped elements exist. The element size is 1 mm. Since the deformation of bridge-type mechanism mainly occurs at flexure hinges, the element size of the hinges is defined as 0.5 mm. The geometrical parameters of the bridge-type mechanism are shown in Fig. 9. In order to enable the comparisons, six samples were set. And the parameters of the material and thickness are shown in Table 1.

The undersurface of link 1 is fixed. Impose 10 μm displacement on the inner surface of link 3 along the reverse direction of X-axis, and 10 μm displacement on the inner surface of link 4 along the X-axis direction. And then the displacement of link 2 is the output displacement of bridge-type mechanism. The results of FEA are shown in Table 2, and Fig. 11 shows the deformation of these six samples. From Table 2, it can be seen that the output displacements and amplification ratios of these six samples are almost the same, only modal frequencies are changed. It verifies the conclusion mentioned in Section 3 that the displacement amplification ratio of the bridge-type mechanism is not related to the material and thickness of the structure.

5. Comparison with existing methods

Eq. (18) is derived by Ma using kinematic principle and virtual work principle [13]. And Eq. (19) is derived by Ye using kinematic principle and elastic beam theory [23]. In this section, comparisons of five methods (Eq. (6), Eq. (17), Eq. (18), Eq. (19) and FEM) are carried out. The results calculated by the FEM can be regarded as true value when the model and the boundary conditions are properly

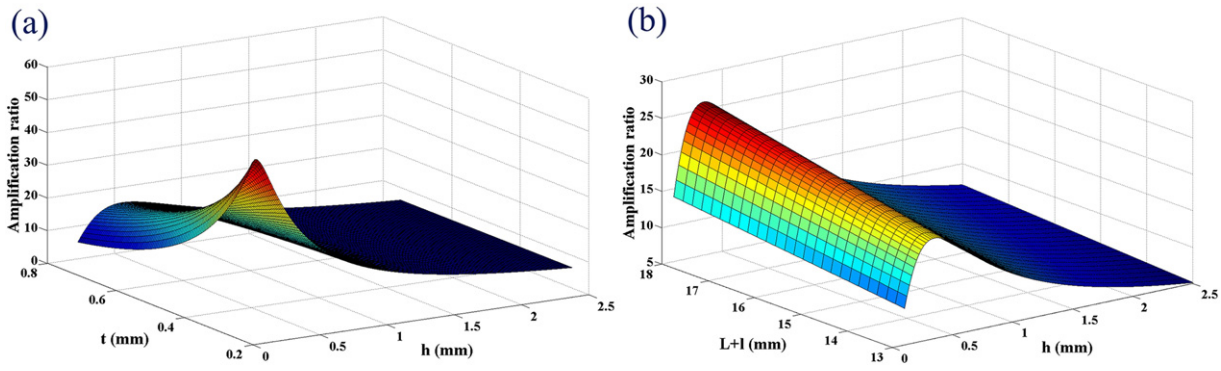

Fig. 10. Relationship between displacement amplification ratio and structural dimensions.

Table 1
Parameters of different samples.

Sample	Elastic modulus (GPa)	Poisson's ratio	Density (kg/mm^3)	b (mm)
1	206	0.27	7.85exp.−6	10
2	71	0.27	2.81exp.−6	10
3	71	0.33	2.81exp.−6	10
4	206	0.27	2.81exp.−6	10
5	71	0.27	2.81exp.−6	8
6	71	0.27	2.81exp.−6	12

prepared. So, in this paper, the displacement amplification ratio calculated by FEM is regarded as the actual displacement amplification ratio.

$$R_{amp\_MA} = \frac{l_a \cos\alpha}{\cos\alpha \dfrac{t^2 \cos\alpha}{6 l_a \sin\alpha} + l_a \sin\alpha} \tag{18}$$

$$R_{amp\_YE} = \frac{\sin\left(\arctan\dfrac{h}{l+L}\right) - \sin\left(\arctan\dfrac{h}{l+L} - \dfrac{6Fhl}{Ebt^3}\right)}{\cos\left(\arctan\dfrac{h}{l+L} - \dfrac{6Fhl}{Ebt^3}\right) - \cos\left(\arctan\dfrac{h}{l+L}\right)} \tag{19}$$

The structural dimensions, which are needed in this section, are shown in Fig. 9. Several non-structural parameters are still required in Eq. (6) and Eq. (19), as shown in Table 3. The relationships between the displacement amplification ratio and dimensions of bridge-type mechanism using different methods are shown in Fig. 12, where *Ramp-ideal*, *Ramp-elastic*, *Ramp-MA*, *Ramp-YE* and *Ramp-FEM* represent the displacement amplification ratio obtained using Eq. (6), Eq. (17), Eq. (18), Eq. (19) and FEM, respectively. There are two things that should be illuminated: in Fig. 12e, the horizontal distance between the centers of hinges was fixed ($L + l = 15.5$ mm); in Fig. 12f, the length of the four arms of bridge-type mechanism was fixed ($L + 2\,l = 18.5$ mm). So, L is changed when l varied, in these two situations.

From Fig. 12a, it can be seen that the curves of *Ramp-elastic*, *Ramp-MA* and *Ramp-FEM* have the same shape. Each of these three curves has a threshold. And after each own threshold, all the three curves descend with the increase of h. Furthermore, the threshold value of *Ramp-elastic* can be derived from Eq. (20).

$$d\left(\frac{3h(l+L)}{t^2+3h^2}\right) \Big/ d(h) = 0 \Rightarrow h = \frac{\sqrt{3}}{3}t \tag{20}$$

From Eq. (20) and Eq. (17)

$$R_{amp\_MAX} = \frac{3 \times \dfrac{\sqrt{3}}{3}t \cdot (l+L)}{t^2 + 3\left(\frac{\sqrt{3}}{3}t\right)^2} = \frac{\sqrt{3}}{2} \cdot \frac{(l+L)}{t} \tag{21}$$

From Eq. (20) and Eq. (21), one can observe that the threshold and peak value of *Ramp-elastic* are related to the width of hinges. However, *Ramp-ideal* and *Ramp-YE* decrease continuously with the increase of h. Furthermore, all these five curves get closer and closer with the increase of h, when h is large enough.

Fig. 12b shows that *Ramp-elastic*, *Ramp-MA* and *Ramp-FEM* decrease when t increases, and *Ramp-FEM* decreases faster than *Ramp-elastic* and *Ramp-MA*. It is mainly caused by two reasons: 1). the applicability of elastic beam theory gets worse when the ratio of t/l increases; 2). the difference of stiffness between hinges and "rigid link" decreases with the increase of t, so the deformation

Table 2
Comparison of results of different samples.

Sample	Maximum nodal stress (MPa)	Output displacement (mm)	First mode (Hz)	Second mode (Hz)	Third mode (Hz)	Fourth mode (Hz)	Amplification ratio
1	102.136	0.144639	190.23	351.30	623.71	684.09	7.23195
2	35.202	0.144639	186.66	344.71	612.01	671.26	7.23195
3	35.783	0.144465	189.77	350.39	615.38	682.20	7.22325
4	102.136	0.144639	317.95	587.17	1042.5	1143.4	7.23195
5	35.228	0.144612	186.45	344.31	516.80	670.46	7.2306
6	35.194	0.144666	186.81	344.98	671.79	705.19	7.2333

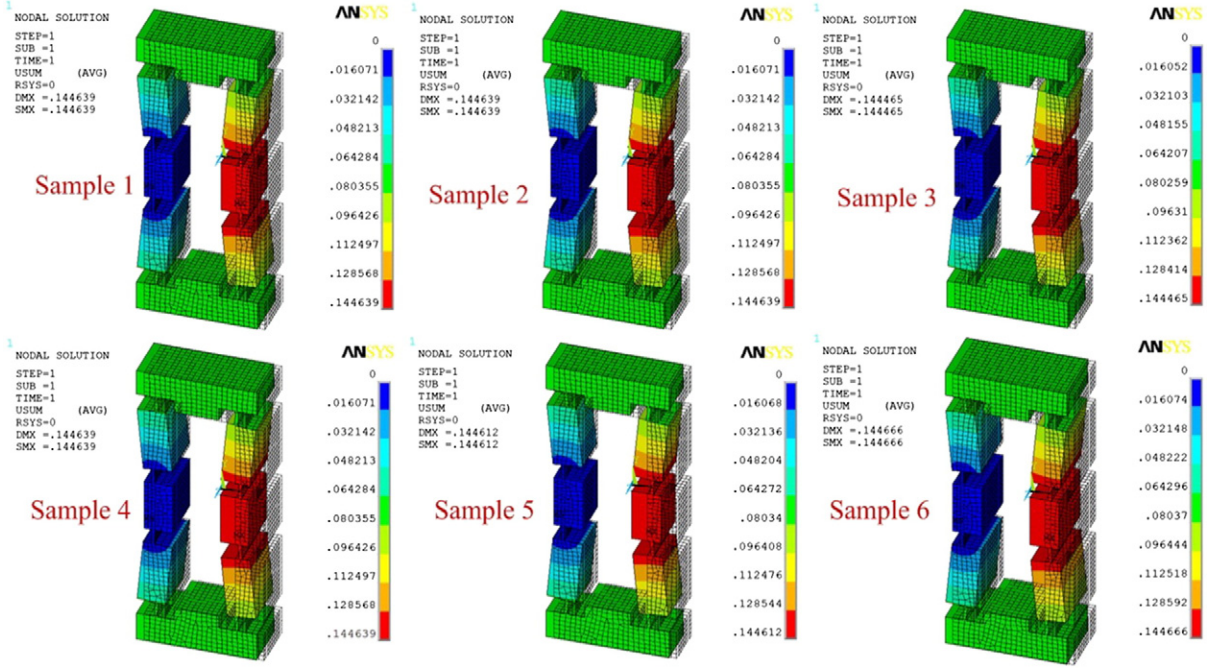

Fig. 11. Deformation of bridge-type mechanism.

of "rigid link" cannot be neglected. Since Eq. (6) has no relationship with the width of hinges, the curve of *Ramp-ideal* is a horizontal line in Fig. 12b.

From Fig. 12c and Fig. 12d, one can observe that *Ramp-ideal*, *Ramp-elastic*, *Ramp-MA*, *Ramp-YE* and *Ramp-FEM* increase with the increase of L and l. The curves of them are linear, and their slopes are almost the same.

From Fig. 12e, it is seen that the all the five curves are almost horizontal lines. So, a conclusion can be drawn: the displacement amplification ratio of bridge-type mechanism is not related to length of hinges when the horizontal distance between the centers of hinges is fixed. Fig. 12f shows that the displacement amplification ratio of bridge-type mechanism decreases with the increase of the length of hinges, when the length of the arms of bridge-type mechanism is fixed.

From all the six charts of Fig. 12, it is easy to see that the curve of *Ramp-elastic* is the nearest one to the curve of *Ramp-FEM*. So, it indicates that Eq. (17) is more accurate than the other formulas. Among all the formulas above, Eq. (3) has the most concise configuration, but the value of it keeps increasing with the decrease of h, and has no limits. Obviously, that is impossible, so its application is limited. Because Eq. (6) is derived from Eq. (3), it also has the same defect. And it can be seen in Fig. 12a. After comparison, it is easy to observe that Eq. (19) is similar to Eq. (1), and the only difference is that the angular displacement is obtained by elastic beam theory in Eq. (19). But the tensile deformation and deflection of hinges are neglected, that means Eq. (19) is not much better than Eq. (1). Besides that, Eq. (19) has another drawback that you should know the input force from the actuator before you use this formula, and that is almost impossible. In addition, the value of F has a great impact on the result of Eq. (19). As mentioned in Section 1, the output displacement of Eq. (18) is obtained only by geometric relations and the elastic deformation was neglected, so its accuracy is debased.

6. Comparisons with previous experiment

Theoretical analysis always has some discrepancies with practice. So, it is very necessary for those analytical formulas to compare with experimental results. There are some experimental works of bridge-type mechanism that have been done by researchers; thus it is very convenient to make this comparison.

Kim et al. [25] designed a long stroke self-guiding stage. This stage is composed by two parallel-connected bridge-type mechanisms and driven by one piezo actuator. And the only difference of these two bridge-type mechanism is the deformation direction, which makes the stage act like a "push–pull train". This form of structure can improve the positioning accuracy of the

Table 3
Non-structural parameters in Eq. (6) and Eq. (19).

	Δx (mm)	F (N)	E (GPa)
Eq. (6)	0.001		
Eq. (19)		10	210

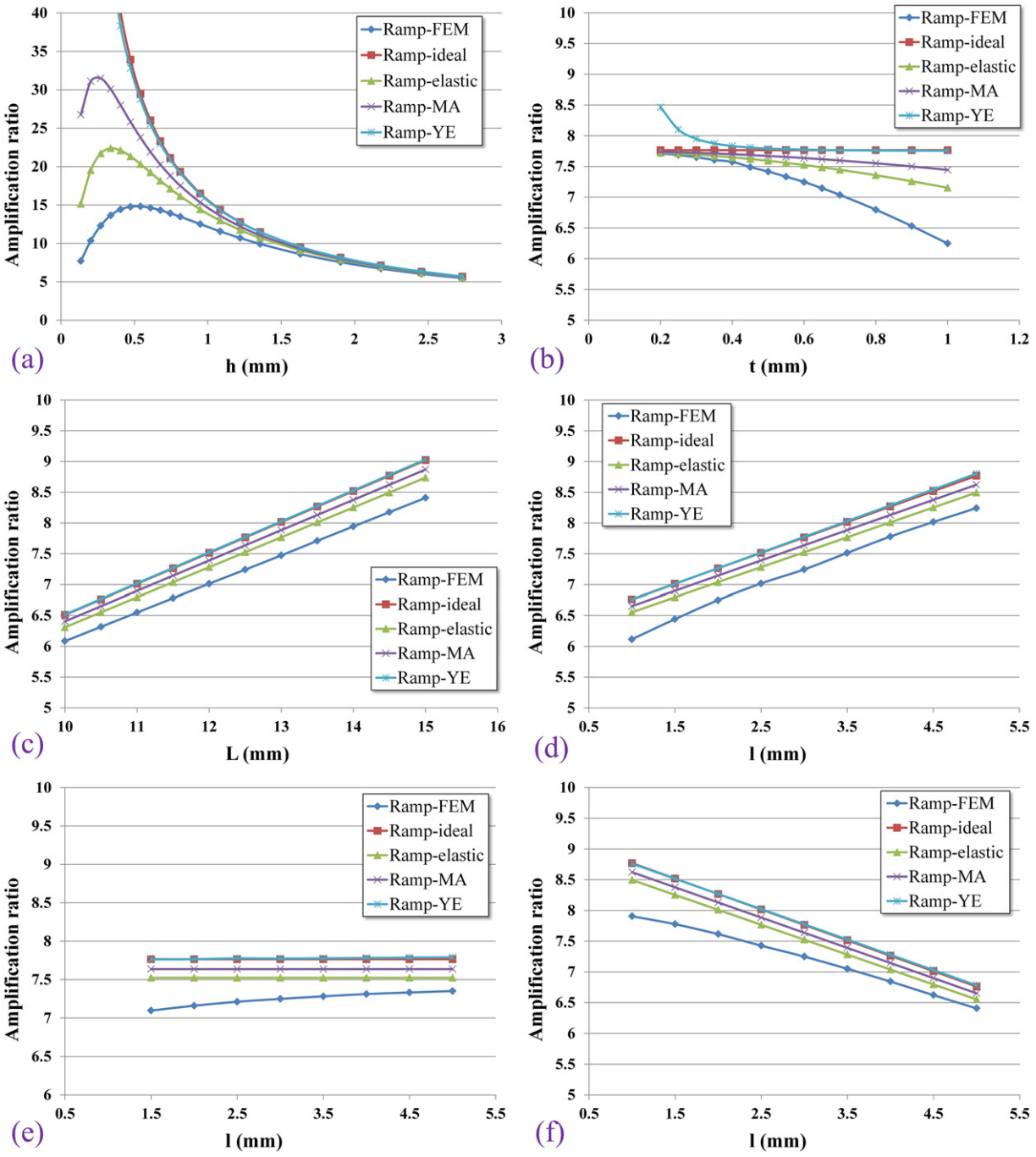

Fig. 12. Comparisons of different methods.

stage, but the displacement amplification ratio of this stage is not doubled, despite the appearance of two bridge-type mechanisms. Actually, this parallel-connected structure makes the displacement amplification ratio of this stage is equal to the displacement amplification ratio of either of the two bridge-type mechanisms. Therefore, the experimental result of Kim's stage is very suitable for this comparison. The structural parameters of the stage are shown in Table 4. And the results of different calculating methods and the experiment are shown in Table 5. There is a thing that should be illuminated in Table 5: the exact driving force from piezo actuator cannot be obtained, so we assume that F in Eq. (19) is 50 N.

From Table 5, it can be seen that the result of FEM is the closest to the experimental result. It means that FEM is the most effective method to predict the displacement amplification ratio of bridge-type mechanism, but the only drawback is its relatively complicated

Table 4
The structural parameters of Kim's stage.

L (mm)	l (mm)	t (mm)	h (mm)	b (mm)
20	3	0.4	1.2	15

process. We can also observe that the result of Eq. (17) is the closest one to the experimental result among the four formulas. It confirms the conclusion of the previous chapter that Eq. (17) is more accurate than the other formulas.

7. Influence of geometric nonlinearity

As mentioned in Section 2, displacement amplification ratio of bridge-type mechanism is a dynamic value in the process of deformation. Along with the deformation of the structure, the vertical distance between the centers of hinges (h) gets smaller and smaller. An estimated relationship can be derived

$$h' = h - \frac{O}{2} \tag{22}$$

where h' represents the vertical distance between the centers of hinges after the deformation, and O represents the output displacement of the bridge-type mechanism. From Eq. (17), it can be seen that displacement amplification ratio is being changed during this process. Moreover, the extreme situation is that h' equals to 0, and then the output displacement will not increase with the increase of the input displacement. It is mainly caused by geometric nonlinearity of the structure. Evidently, it's related to input displacement. And this phenomenon becomes obvious, when the input displacement gets relatively large. So, large deformation analysis should be taken. This nonlinear static analysis is also realized by ANSYS11.0, and the finite element model is the same as sample 2 which is used in Section 4. In order to find out the influence of geometric nonlinearity, result comparison between linear static analysis and nonlinear static analysis is shown in Table 6.

From Table 6, it is easy to observe that the difference between the amplification ratios obtained from these two kinds of analysis increases with the increase of the input displacement. But the difference is quite small, when the input displacement is relatively small. From Eq. (22), h' is about 1.73 mm when the input displacement is 70 μm, since h is 2 mm in this finite element model. From Fig. 12a, the amplification ratio increases continuously when h decreases from 2 mm to 1.73 mm. So, the amplification ratios obtained from nonlinear static analysis is actually the even amplification ratio of the whole process of deformation. Assume that h equals to the threshold of *RampFEM* in Fig. 12a, and then the amplification ratio reaches its peak. But the output displacement won't be as large as expected, when the input displacement is relatively large. That is because the amplification ratio descends with the decrease of h, when h is smaller than the threshold. So, the amplification ratio is not the larger the better, when designing the bridge-type mechanism. The input displacement and the trend of the amplification ratio during the deformation should be considered too.

8. Conclusions

The kinematic characteristics of bridge-type mechanism are analyzed, and the average ideal displacement amplification ratio of the deformation process is obtained by means of integral. Elastic beam theory is used to derive the theoretic displacement amplification ratio of bridge-type mechanism. The relationship between displacement amplification ratio and dimensions of bridge-type mechanism is deeply analyzed. Comparisons with existing methods have been made. In order to confirm the conclusion reached in this paper, comparison with previous experimental results has also been made. Moreover, the influence of geometric nonlinearity of bridge-type mechanism is well analyzed in this paper.

From the above analysis, the following conclusions can be drawn:

(1) The displacement amplification ratio of bridge-type mechanism is not related to the material and thickness of the structure. It is only determined by planar dimensions of the structure.
(2) The vertical distance between the centers of hinges is the most sensitive structural parameter of bridge-type mechanism. As it increases from zero, the displacement amplification ratio increases quite fast until it reaches the peak, and then decreases slowly. And the threshold and the peak are related to the width of hinges.
(3) The displacement amplification ratio bridge-type mechanism is not related to the respective length of “rigid link” and flexure hinges, but the sum length of them. And the displacement amplification ratio increases with the increase of their sum length.

Table 5
The results of different calculating methods and the experiment.

	Eq. (6)	Eq. (17)	Eq. (18)	Eq. (19)	FEM	Experiment
Displacement amplification ratio	30.593	18.482	18.819	22.497	15.43	12.025

Table 6
Result comparison between linear static analysis and nonlinear static analysis.

Input displacement (μm)	Output displacement of linear static analysis (μm)	Output displacement of nonlinear static analysis (μm)	Amplification ratio of linear static analysis	Amplification ratio of nonlinear static analysis
10	72.320	72.956	7.2320	7.2956
20	144.639	146.928	7.2320	7.3464
30	216.959	221.946	7.2320	7.3982
40	289.279	298.043	7.2320	7.4511
50	361.598	375.253	7.2320	7.5051
70	506.238	533.146	7.2320	7.6164

(4) Due to the geometric nonlinearity of bridge-type mechanism, the displacement amplification ratio of bridge-type mechanism will be influenced by the input displacement during the procedure of deformation. But the influence could be ignored when the input displacement is quite small.

Acknowledgment

This work was supported by the 02 Major National Science and Technology Projects of China (2009ZX02202-005).

References

[1] Y. Tian, B. Shirinzadeh, D. Zhang, A flexure-based mechanism and control methodology for ultra-precision turning operation, Precis. Eng. 33 (2) (2009) 160–166.
[2] V. F. Paz, S. Peterhänsel, K. Frenner, W. Osten, Solving the inverse grating problem by white light interference Fourier scatterometry, Light: Science & Applications http://dx.doi.org/10.1038/lsa.2012.36
[3] W. Xiong, Y.S. Zhou, X.N. He, Y. Gao, M. Mahjouri-Samani, L. Jiang, T. Baldacchini, Y.F. Lu, Simultaneous additive and subtractive three-dimensional nanofabrication using integrated two-photon polymerization and multiphoton ablation, Light: Science & Applications http://dx.doi.org/10.1038/lsa.2012.6
[4] Q. Yao, J. Dong, P.M. Ferreira, Design, analysis, fabrication and testing of a parallel-kinematic micropositioning XY stage, Int. J. Mach. Tools Manuf. 47 (2007) 946–961.
[5] J. Juuti, K. Kordás, R. Lonnakko, V.-P. Moilanen, S. Leppävuori, Mechanically amplified large displacement piezoelectric actuators, Sensors Actuators A 120 (2005) 225–231.
[6] K.-B. Choi, J.J. Lee, S. Hata, A piezo-driven compliant stage with double mechanical amplification mechanisms arranged in parallel, Sensors Actuators A 125 (2010) 173–181.
[7] Y.-J. Choi, S.V. Sreenivasan, B.J. Choi, Kinematic design of large displacement precision XY positioning stage by using cross strip flexure joints and over-constrained mechanism, Mech. Mach. Theory 43 (2008) 724–737.
[8] H.C. Liaw, B. Shirinzadeh, Robust generalised impedance control of piezo-actuated flexure-based four-bar mechanisms for micro/nano manipulation, Sensors Actuators A 148 (2008) 443–453.
[9] Y. Yue, F. Gao, X. Zhao, Q.J. Ge, Relationship among input-force, payload, stiffness and displacement of a 3-DOF perpendicular parallel micro-manipulator, Mech. Mach. Theory 45 (2010) 756–777.
[10] Z. Ni, D. Zhang, Y. Wu, Y. Tian, M. Hu, Analysis of parasitic motion in parallelogram compliant mechanism, Precis. Eng. 34 (2010) 133–138.
[11] M. Jouaneh, R.Y. Yang, Modeling of flexure-hinge type lever mechanisms, Precis. Eng. 27 (2003) 407–418.
[12] C.-L. Chu, S.-H. Fan, A novel long-travel piezoelectric-driven linear nanopositioning stage, Precis. Eng. 30 (2006) 85–95.
[13] H.-W. Ma, S.-M. Yao, Li-Q. Wang, Z. Zhong, Analysis of the displacement amplification ratio of a bridge-type flexure hinge, Sensors Actuators A 132 (2006) 730–736.
[14] W. Xu, T. King, Flexure hinges for piezoactuator displacement amplifiers: flexibility, accuracy, and stress considerations, Precis. Eng. 19 (1996) 4–10.
[15] Y. Tian, B. Shirinzadeh, D. Zhang, G. Alici, Development and dynamic modeling of a flexure-based Scott–Russell mechanism for nano-manipulation, Mech. Syst. Signal Process. 23 (2009) 957–978.
[16] J.H. Kim, S.H. Kim, Y.K. Kwak, Development and optimization of 3-D bridge-type hinge mechanisms, Sensors Actuators A 116 (2004) 530–538.
[17] Q. Xu, Y. Li, Analytical modeling, optimization and testing of a compound bridge-type compliant displacement amplifier, Mech. Mach. Theory 46 (2011) 183–200.
[18] Y. Tian, B. Shirinzadeh, D. Zhang, Y. Zhong, Three flexure hinges for compliant mechanism designs based on dimensionless graph analysis, Precis. Eng. 34 (2010) 92–100.
[19] N. Lobontiu, J.S.N. Paine, E. Garcia, M. Goldfarb, Design of symmetric conic-section flexure hinges based on closed-form compliance equations, Mech. Mach. Theory 37 (2002) 477–498.
[20] Y. Tian, B. Shirinzadeh, D. Zhang, Closed-form compliance equations of filleted V-shaped flexure hinges for compliant mechanism design, Precis. Eng. 34 (2010) 408–418.
[21] B.J. Pokines, E. Garcis, A smart material microamplification mechanism fabricated using LIGA, Smart Mater. Struct. 7 (1998) 105–112.
[22] N. Lobontiu, E. Garcia, Analytical model of displacement amplification and stiffness optimization for a class of flexure-based compliant mechanisms, Comput. Struct. 81 (2003) 2797–2810.
[23] G. Ye, W. Li, Y.-Q. Wang, X.-F. Yang, L. Yu, Kinematics analysis of bridge-type micro-displacement mechanism based on flexure hinge, Proceedings of the 2010 IEEE International Conference on Information and Automation, 2010, pp. 66–100.
[24] Y. Koseki, T. Tanikawa, T. Arai, N. Koyachi, Kinematic analysis of translational 3-DOF micro parallel mechanism using matrix method, Proceedings of the 2000 IEEE/RSJ International Conference on Intelligent Robots and Systems, 2000, pp. 786–792.
[25] J.-J. Kim, Y.-M. Choi, D. Ahn, B. Hwang, D.-G. Gweon, J. Jeong, A millimeter-range flexure-based nano-positioning stage using a self-guided displacement amplification mechanism, Mech. Mach. Theory 50 (2011) 109–120.